

The Effect of Temperature on the Creep Ageing Characteristics of Al-Li Alloys

Tong Feng¹, Bolin Ma¹, Fei Chen¹, Lihua Zhan^{1,2,*}, Yongqian Xu^{1,*} and Chunyu Yang¹

¹Light Alloy Research Institute of Central South University, Changsha, 410083, China

²School of Mechanical and Electrical Engineering, Central South University, Changsha, 410083, China

Abstract: In this paper, the evolution of creep strain and mechanical properties of 2195 Al-Li alloy is investigated at different temperatures (160/170/180°C), with the aim of discovering the mechanism of temperature influence on creep properties and providing a reference for improving the creep properties of the target material by adjusting the temperature in the future. This study demonstrates that the creep curve is strongly influenced by temperature, with a plateau and a transition period occurring at low temperatures. As the temperature increases, the creep curve gradually reverts to the typical two-stage creep characteristics due to the interaction of dislocation density proliferation and dislocation reversion within the material at high temperatures. In addition, by means of tests such as TEM, it was confirmed that the decrease in mechanical properties of the material caused by increasing the creep temperature is mainly due to the coarsening of precipitates and the appearance of precipitation-free zones at grain boundaries.

Keywords: Al-Li alloy, Creep aging, Mechanical properties, Microstructure evolutions, Temperature.

1. INTRODUCTION

With the development of the aviation industry, the requirements for the performance of space vehicles are increasing and the requirements for structural materials are also increasing day by day. Aluminium alloys are widely used in the aerospace industry because of their low density, good corrosion resistance and ease of processing. And with the development of society, further increases in payload and voyage of space vehicles are the way forward. As a representative of lightweight and high-strength structural materials, aluminium-lithium alloy not only has the advantages of traditional Al alloys, but also has lower density and higher strength, and is gradually replacing traditional Al alloys in aerospace manufacturing applications [1-3]. As previously reported, for every 1% increase in Li element in Al-Li alloys, the alloy density decreases by 3% and the alloy modulus of elasticity increases by 6% [4]. However, in actual manufacturing, Al-Li alloy components are difficult to shape precisely, especially during the manufacture of large components where springback is more pronounced. As an advanced manufacturing process developed specifically for the manufacture of large Al alloy components, creep-age forming (CAF) involves creep forming and stress ageing processes [5]. Large Al alloy components can be formed and strengthened simultaneously by the corresponding creep/stress relaxation and age strengthening to meet the practical requirements.

In recent years, researchers have studied the changes in the microstructure of Al alloys during creep aging process by means of characterisation techniques such as TEM, revealing the relationship between microstructure and creep properties, which in turn has promoted the development of CAF [6-9]. Dong [10] *et al.* and Tang [11] *et al.* evaluated the effect of pre-deformation on the creep ageing process of Al alloys and showed that the increase in pre-deformation strain can promote the ageing precipitation process and improve the tensile properties, Kahn tearing properties and fatigue extension properties of the formed alloy at room temperature; at the same time, increasing pre-deformation will bring a large number of dislocations to the lattice, which can be detached from the pinning effect of the reinforced precipitates under the stress field, promoting creep strain and improving creep strength. Yang [12] *et al.* found that 5% and 7% strain improved creep strain, with reversal occurring when the strain went to 9%. The work presented by Chen [13] *et al.* showed that the loading rate accelerates the creep process by changing the initial behaviour, making the plastic deformation increase during the loading phase, which in turn affects the final deformation and the microstructure of the material, but the loading rate does not have a direct effect on the creep mechanism. Xu [14] *et al.* carry out the experiments on the creep behaviour of Al-Cu-Mg alloy at different temperature rise rates, and the results showed that with the increase of the temperature rise rate, the creep deformation, yield strength and tensile strength of the material decreased during the heating process; meanwhile, the size of grain boundary precipitates and the width of precipitation-free zone also increased with

*Address correspondence to this author at the Light Alloy Research Institute of Central South University, Changsha, 410083, China; Tel: +86-13974874472; E-mail: yjs-cast@csu.edu.cn; yongqian.xu@csu.edu.cn

the increase of the temperature rise rate. Xu [15] *et al.* and Chen [16] *et al.* explored the effect on creep behaviour during a two-stage creep ageing process. Xu *et al.* found that temperature was the main influence on creep behaviour during two-stage creep ageing. Chen *et al.* proposed that two-stage creep aging would allow the elongation of Al-Li alloys to increase without a reduction in strength or creep strain. Zhan [17] *et al.* then explored the different creep ageing behaviour under elastic loading and plastic loading, showing that under elastic loading the creep deformation behaviour exhibits multi-stage creep characteristics, while under plastic loading the creep behaviour exhibits a typical two-stage behaviour.

Chen [18] and Chen [19] *et al.* tuned the creep properties of Al-Li alloys by adding a period of pre-aging behaviour prior to creep aging, demonstrating that pre-aging can effectively increase elongation without reducing strength, while also promoting a shift in fracture mechanism from intergranular fracture to mixed fracture. Zhou [20] *et al.* used electrical pulses to adjust the creep properties of Al-Cu-Li during creep ageing and found that the introduction of electrical pulses at the initial stage of creep could promote dislocation movement making the creep strain increase, and the application of electrical pulses at the final stage induced an increase in elongation. The results of work conducted by Zhou and Chen [21-22] *et al.* showed that as the frequency of electrical pulses increased, dynamic recrystallisation was promoted and the average grain size became smaller, therefore resulting in improved creep ageing formability and mechanical properties of the alloy. Wang [23] *et al.* proposed a mechanism-based creep intrinsic structure

model and combined it with the work-hardening equation to accurately describe the creep deformation of the T8 state Al-Li alloy from 0.02% to 0.45%. Peng [24] *et al.* established a unified intrinsic structure model for the anisotropy of Al-Li alloys and successfully described the creep ageing behaviour of AA2195 Al-Li alloy. In most studies, process parameters such as pre-strain, pre-aging, electrical pulses etc. have been adjusted to influence the properties of dislocations and precipitates and the mechanical properties of the material. However, little research has been carried out on some of the problems of 2195 Al-Li alloy in the forming process, such as the poor plasticity of the aged Al-Li alloys at high temperature. These problems to a certain extent limit the application of creep ageing processes in practical production.

Using 2195-T34 Al-Li alloy as the target material, the creep behaviour at 160/170/180°C and the differences in mechanical properties and microstructural changes after creep aging were investigated, with the aim of discovering the influence of temperature on the properties of the material after creep aging and the reasons for its occurrence, and providing a reference for the subsequent creep aging process of Al-Li alloy.

2. EXPERIMENTAND METHODS

2.1. Materials and Specimens

Table 1 illustrates the material parameters of the T34Al-Li alloy used in this study. The pattern required in this study was cut along the rolling direction of the sheet and Figure 1 illustrates the shape and dimensions of the specimens used.

Table 1: The Element Composition of the 2195 Al-Li Alloy (wt.%)

Element composition	Cu	Li	Mg	Ag	Fe	Zr	Mn	Si	Ti	Al
Weight fraction	4.18	1.19	0.40	0.38	0.052	0.094	0.0047	0.014	0.018	Bal.

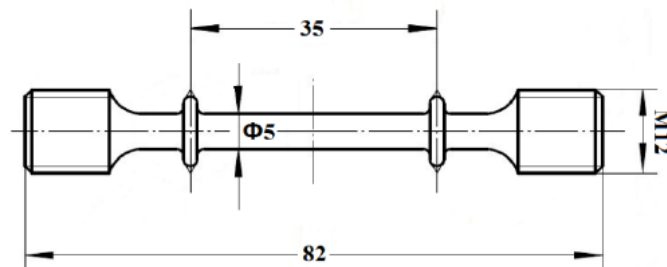


Figure 1: Dimensions of the sample (unit: mm).

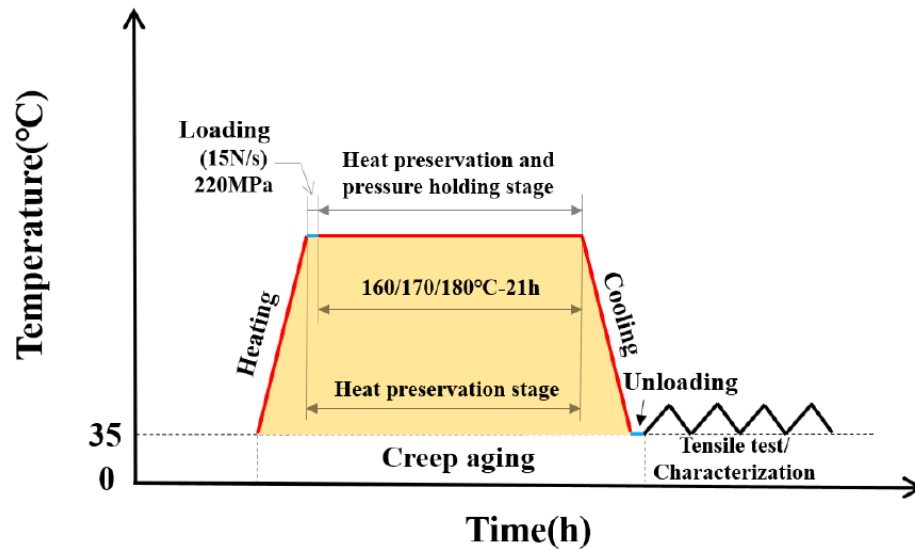


Figure 2: Experimental programme and flow.

2.2. Experimental Programme

The experiments were divided into three groups: the material was held at 160/170/180°C for 21 h respectively and the specimens were subjected to a stress of 220 MPa. After the specimen is mounted to the creep machine, a preload force of 200 N is applied to the specimen to eliminate the mounting and connection gap, then heating of the specimen is started at a rate of 5°C/min. After the temperature of the specimen reaches the target temperature (160/170/180°C) holding is started and loading is started at a rate of 15 N/s until the stress applied to the specimen reaches the target value (220 MPa) and is maintained. When the holding time reaches 21 h, the specimen is unloaded and cooled down to remove the sample. At the same time, intermittent experiments are carried out in order to explore the evolution of the mechanical properties of the material as it progresses through the ageing tests. The specific experimental programme is arranged as shown in Figure 2. It should be noted that the yield strength of the target material at 160-180°C is approximately 240-250 MPa and that creep ageing at a stress of 220 MPa is in the elastic state.

2.3. Mechanical Properties Test and Microstructural Characterisation

In this paper, the yield strength, ultimate tensile strength and elongation of the patterns were tested using an MTS tensile machine at a speed of 2mm/min. At least two samples of each type of the same heat treatment were selected for testing to ensure the accuracy of the experimental data.

The Tescan mira3 field emission scanning electron microscope (SEM) was used to observe the fracture surface of the specimen after stretching. The microstructure of the samples at different stages was observed by transmission electron microscopy (TEM). The specimens were ground to a thickness of 80 μm and then a punch was used to obtain \varnothing 3mm discs. The discs were twin-jet electro polished at -30°C using a mixture made from 25% nitric acid and 75% alcohol. The TEM samples were examined on TalosF200X equipment operating at 300 KV. XRD testing with the Advance D8 X-ray diffractometer, scanning a range of 20°-90° at 2° per minute.

3. RESULTS AND DISCUSSION

3.1. Creep Behaviour

Figure 3 shows the creep curves at different temperatures, from which it is clear enough that temperature has a more pronounced effect on the creep properties of the target alloy. As the temperature increases, the creep strain also progressively increases, with no significant difference in the final steady state rate. At 160°C, creep ageing has a clear plateau at A in the diagram, while only a transition period at B exists when the temperature rises to 170°C. When the temperature rises to 180°C again, the creep curve shows the typical two-stages creep characteristic [25-26], with no plateau or transition period present. It is well known that creep strain arises from the movement of dislocations, and that creep behaviour causes changes in dislocations, which is a complex interplay of dynamic processes [27-28]. In order to

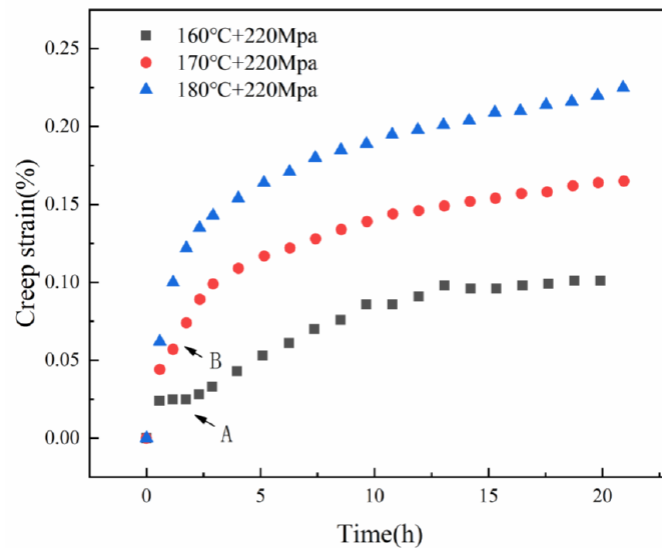


Figure 3: Creep curves at different temperatures.

further understand the mechanism behind this phenomenon, it is necessary to understand the dislocation density within the material.

As illustrated in Figure 4(a), X-ray diffraction (XRD) analysis was carried out on specimens at 3h and 21h in order to fully understand the variation of dislocation density with the creep process at different temperatures for the 2195 Al-Li alloy. X-ray peaks can

reflect the condition of defects (dislocations) present in the internal crystal structure of a material, and an increase in the density of dislocations in a crystal increases the X-ray full width at half maximum (FWHM) [29-30]. Figure 4(b) and (c) show the full width at half maximum of the XRD diffraction curves of creep specimens at different angles of diffraction for 3h and 21h of aging at different temperatures, respectively.

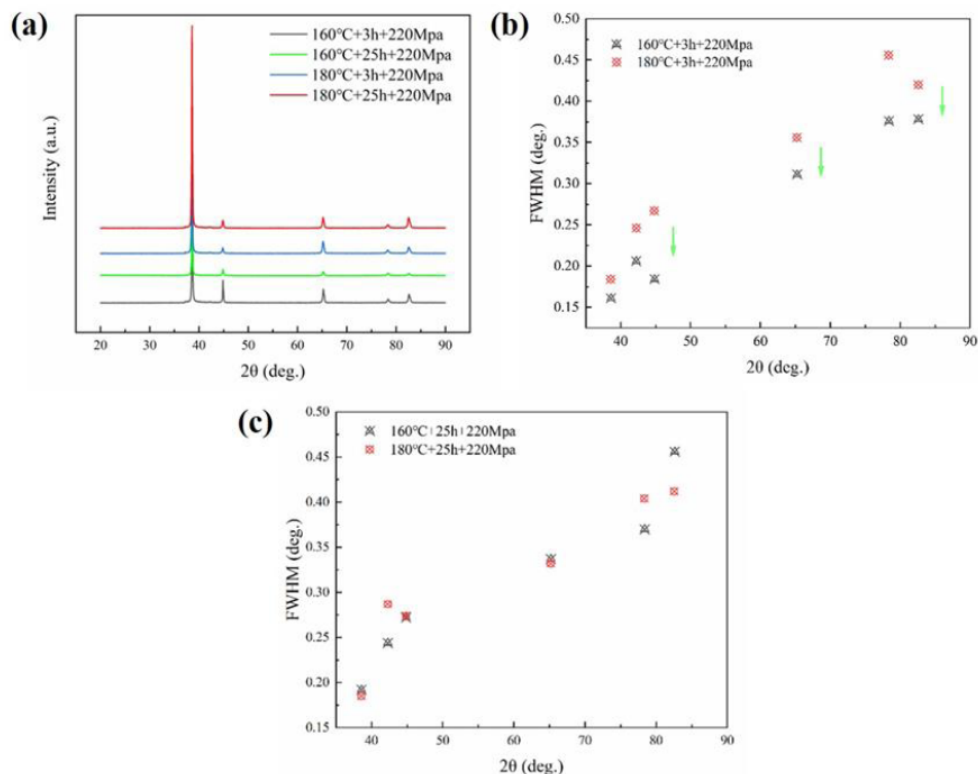


Figure 4: XRD patterns (a) and FWHM at different moments (b-c).

Not only that, but the wave peaks of the diffraction curves obtained by XRD also represent different precipitates [31]. The number and position of the wave peaks in all four diffraction curves in Figure 4(a) remain the same, indicating that there is no difference in the type of precipitates within the material at 160°C and 180°C for 3h and 21h of creep aging, suggesting that the sequence of precipitates and the type of precipitates are not affected when the temperature is varied within a certain range. The FWHM for creep at 160°C and 180°C for 3h is shown in Figure 4(b). It can be seen that the values of FWHM at 160°C are both higher than the FWHM at 180°C, indicating that: the dislocation density of the material after creep for 3h at 160°C is lower than that at 180°C for the same creep time. The FWHM for samples aged at 160°C and 180°C for 21h is shown in Figure 4(c). The figure shows that the difference between the value of FWHM at a temperature of 160°C and the FWHM at a temperature of 180°C when aged 21h is not significant, indicating that: the difference in dislocation density between the two groups of specimens at creep temperatures of 160°C and 180°C is large at 3h, and the difference in dislocation density narrows as creep progresses. It is worth noting that the dislocation density of the specimens with a creep temperature of 180°C is higher than that of the specimens with a creep temperature of 160°C at 3h. In general, an increase in temperature speeds up the annihilation rate of dislocations and decreases the dislocation density [32], but why would a higher creep temperature here result in a higher dislocation density? This is probably due to the lower activation energy of dislocations at high temperatures, the creep strain is more considerable within the initial phase of creep, and new dislocation proliferation occurs during the creep process,

increasing the dislocation density, which in turn increases the creep strain, ultimately leading to a creep curve at 180°C with no plateau and transition period, whereas at low temperatures, the opposite is true, leading to a plateau in the creep curve. As creep progresses, the groups of specimens enter a steady-state creep phase where dislocation strengthening and reversionary softening reach equilibrium and are no longer temperature sensitive, leading to a reduction in the dislocation density difference between the groups of specimens at a later stage.

3.2. Mechanical Strength

Figure 5 shows the variation of creep ageing strength and elongation of the specimens at 160/170/180°C. The trend of the different performance curves in Figure 5(a) and 5(b) shows that the creep specimen at 180°C has reached its peak ageing state at 3 h; The creep specimen at 160/170°C reaches its peak ageing stage at 9 / 6 h respectively. With the increase of aging temperature, the peak aging strength decreased. As the ageing time increases, the strength of the 160/170°C specimens fluctuates little and tends to rise slightly, while the 180°C specimens show a certain downward trend in yield strength after a short plateau period of peak ageing. The yield strengths of the three sets of specimens at 21 h creep were 580, 577 and 554 MPa respectively.

The change in elongation for the three sets of specimens is presented in Figure 5(c), where the trend in elongation is opposite to the trend in strength. After aged 3h, the elongation of the 160/170 °C creep specimens did not fluctuate much, with elongation rates of 7.5 % and 7 % respectively. The 180°C specimens showed little overall change with time after 6 h of

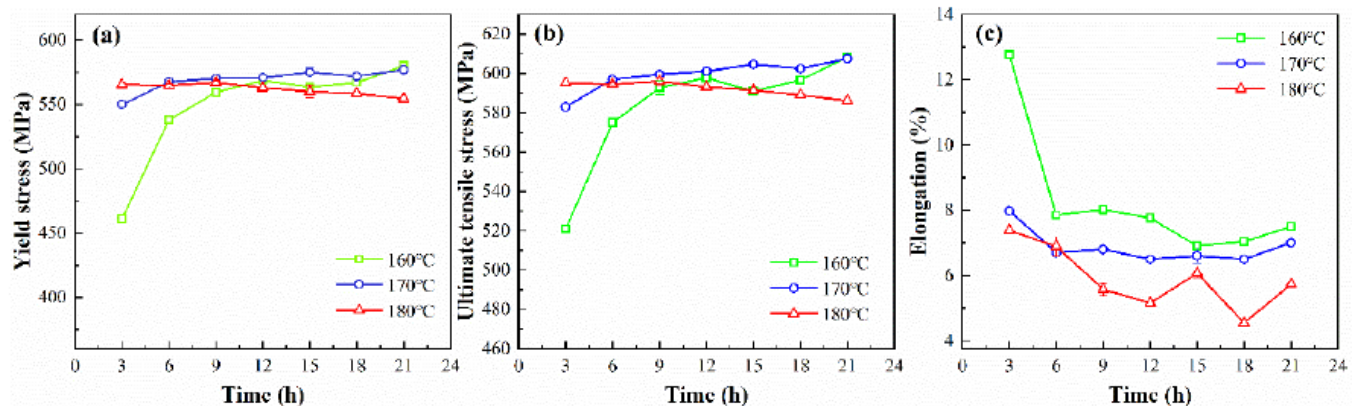


Figure 5: Variation of creep mechanical properties with time at different temperatures.

creep. At an aging time of 21 h, the elongation of the 180°C specimen was 5.6%.

The above results show that an increase in temperature significantly promotes ageing, but reduces peak ageing strength and elongation. Changes in macroscopic properties are necessarily a result of changes in microstructure, and the microstructure of creep at different temperatures will be discussed below.

Figure 6 shows the intracrystalline precipitates of the specimens after creep aging at 160/180°C for 21h. It can be seen that the main precipitates in the two groups of different specimens are T1 phase and less θ' phase. Comparing the two graphs in Figure 6(a) and Figure 6(b), it can be found that the T1 phase of the precipitate is more elongated at 160°C; the T1 phase becomes significantly thicker at 180°C temperature. The coarsening of the precipitates triggers a gradual change of the dislocation mechanism from a cut-through mechanism to a bypass mechanism, weakening the impeding effect of the precipitates on the dislocation movement and reducing the strengthening effect [33]. In addition, the coarsening of the precipitates indicates that the heat treatment state of the specimen is changing from peak ageing to over-ageing, which reduces the overall properties of the material, including strength and elongation, in line with the trend in mechanical properties in Figure 5. It can be seen that the increase in ageing temperature reduces the strength plasticity due to the coarsening of the precipitates.

Grain boundaries are closely related to the elongation of the material, and the appearance of precipitation-free bands at grain boundaries can lead to brittle fracture of the material, causing a significant reduction in plasticity [34-36]. Figure 7 shows the intergranular microstructure of the specimen after creep ageing for 21h at 160/180°C. In Figure 7(a) (160°C) many fine, dense precipitates are visible near the grain boundaries and there are no obvious precipitation-free zones at the grain boundaries. This phenomenon has not been found in previous research work either. Ren *et al.* [37] point out that at lower temperatures the precipitation power of the precipitating phase is high and the required concentration of critical vacancies decreases, so that precipitates are formed when vacancies near the grain boundary diffuse towards the grain boundary and no obvious precipitation-free zone at the grain boundary can be observed. When the temperature increases, the vacancy diffusion to the grain boundary is accelerated, but the critical vacancy concentration required for precipitation also increases, and there is a wider region near the grain boundary where the vacancy concentration is less than the critical vacancy concentration required for precipitation, resulting in the appearance of no precipitation zone or no precipitation band broadening at the grain boundary [38]. In addition, the intracrystalline precipitates in Figure 7(a) are clearly finer than those in Figure 7(b), in keeping with the comparison of the intracrystalline precipitates characteristics in the previous section. The above shows that the decrease in performance caused by the increase in temperature is due to the change in

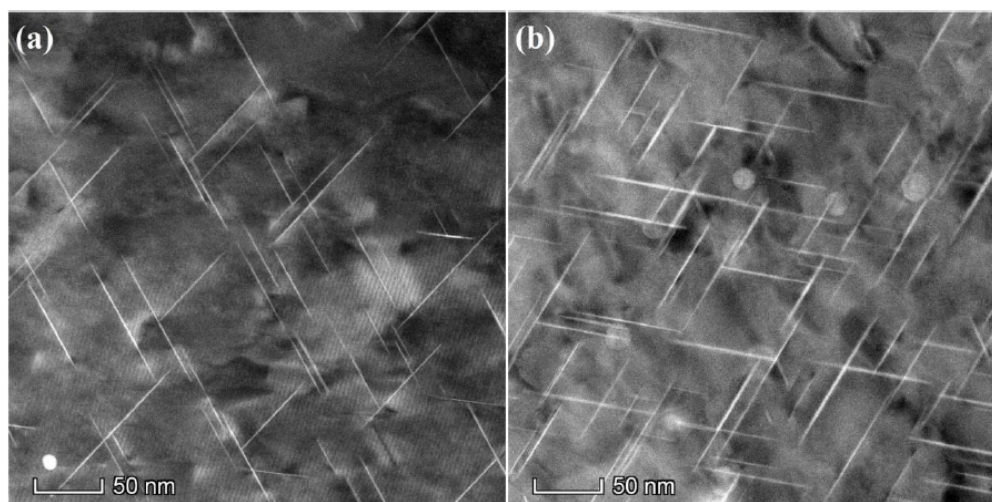


Figure 6: Intracrystalline precipitates of specimens aged at 160°C (a) and 180°C (b) for 21h.

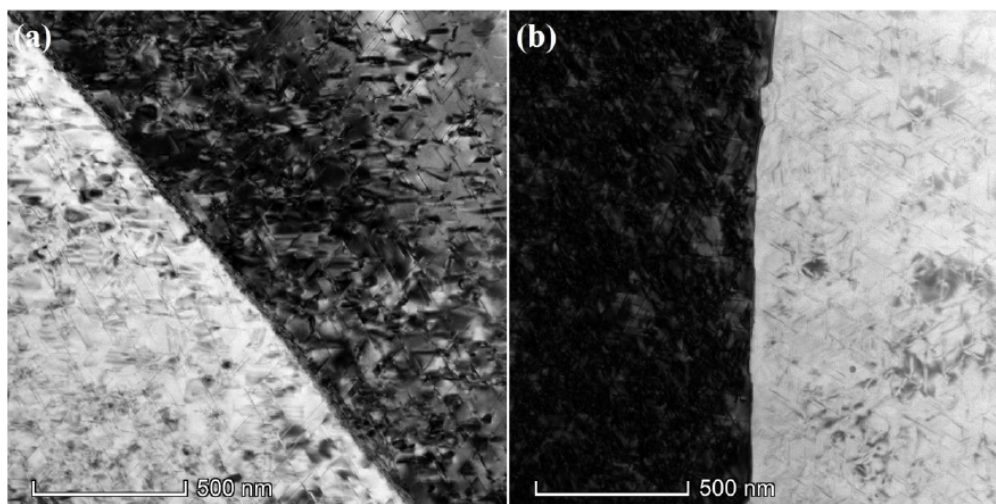


Figure 7: Grain boundary microstructure of specimens aged at 160°C (a) and 180°C (b) for 21h.

precipitates and precipitate-free zones caused, specifically: the reason for better performance at low temperatures is that the precipitates are finer and denser at this time; the increase in temperature coarsens the precipitates, causing a reduction in strengthening and poor plasticity.

5. CONCLUSION

In this paper, the effect of temperature on creep ageing properties was investigated. Focusing on how temperature affects tensile strength and elongation in terms of strength, elongation and microstructure, the following conclusions are listed.

(1) As the temperature increases, the plateau or transition period in the creep curve will disappear due to the interaction of dislocation density proliferation and dislocation recovery within the material at high temperatures.

(2) The overall performance of Al-Li alloys after creep aging decreases with increasing temperature, including strength and elongation.

(3) Increasing the temperature reduces the peak strength of creep aging of Al-Li alloys, and gradually decreases with the extension of the aging time, mainly because the increase in temperature promotes the coarsening of precipitates.

(4) The reasons for the decrease in elongation caused by the increase in temperature are the transformation of the material to the over-aged state

and the appearance of precipitation-free zones at grain boundaries.

DECLARATION OF INTEREST STATEMENT

The authors state that there is no interest dispute or other competitive relationship in this work.

REFERENCES

- [1] Wang X, Wang J, Yue X, *et al.* Effect of aging treatment on the exfoliation corrosion and stress corrosion cracking behaviors of 2195 Al-Li alloy [J]. *Materials & Design*, 2015; 67: 596-605. <https://doi.org/10.1016/j.matdes.2014.11.007>
- [2] Ning J, Li Q, Zou Z, *et al.* Hot tensile deformation behavior and microstructural evolution of 2195 Al-Li alloy [J]. *Vacuum*, 2021; 188: 110176. <https://doi.org/10.1016/j.vacuum.2021.110176>
- [3] Ma Y, Li J, Sang F, *et al.* Grain structure and tensile property of Al-Li alloy sheet caused by different cold rolling reduction [J]. *Transactions of Nonferrous Metals Society of China*, 2019; 29(8): 1569-1582. [https://doi.org/10.1016/S1003-6326\(19\)65064-8](https://doi.org/10.1016/S1003-6326(19)65064-8)
- [4] Li Q, Ning J, Chen L, *et al.* The mechanical response and micro structural evolution of 2195 Al-Li alloy during hot tensile deformation [J]. *Journal of Alloys and Compounds*, 2020; 848: 156515. <https://doi.org/10.1016/j.jallcom.2020.156515>
- [5] Xu L, Zhan L, Xu Y, *et al.* Thermo mechanical pretreatment of Al-Zn-Mg-Cu alloy to improve formability and performance during creep-age forming [J]. *Journal of Materials Processing Technology*, 2021; 293: 117089. <https://doi.org/10.1016/j.jmatprotec.2021.117089>
- [6] Li H, Huang D, Kang W, *et al.* Effect of different aging processes on the microstructure and mechanical properties of a novel Al-Cu-Li alloy [J]. *Journal of Materials Science & Technology*, 2016; 32(10): 1049-1053. <https://doi.org/10.1016/j.jmst.2016.01.018>
- [7] Lei C, Yang H, Li H, *et al.* Dependences of microstructures and properties on initial tempers of creep aged 7050 aluminum alloy [J]. *Journal of Materials Processing*

- Technology, 2017; 239: 125-132.
<https://doi.org/10.1016/j.jmatprotec.2016.07.004>
- [8] Wang Y L, Jiang H C, Li Z M, *et al.* Two-stage double peaks ageing and its effect on stress corrosion cracking susceptibility of Al-Zn-Mg alloy [J]. *Journal of materials science & technology*, 2018; 34(7): 1250-1257.
<https://doi.org/10.1016/j.jmst.2017.05.008>
- [9] Jiang B, Cao F, Wang H, *et al.* Effect of aging time on the microstructure evolution and mechanical property in an Al-Cu-Li alloy sheet [J]. *Materials Science and Engineering: A*, 2019; 740: 157-164.
<https://doi.org/10.1016/j.msea.2018.10.064>
- [10] Dong Y, Ye L, Liu X, *et al.* Effects of large strain pre-deformation on creep age behavior and microstructural evolution of an Al-Cu-Li alloy [J]. *Materials Letters*, 2022, 324: 132699.
<https://doi.org/10.1016/j.matlet.2022.132699>
- [11] Tang J, Bo Y U, Zhang J, *et al.* Effects of pre-deformation mode and strain on creep aging bend-forming process of Al-Cu-Li alloy [J]. *Transactions of Nonferrous Metals Society of China*, 2020, 30(5): 1227-1237.
[https://doi.org/10.1016/S1003-6326\(20\)65291-8](https://doi.org/10.1016/S1003-6326(20)65291-8)
- [12] Yang X, Wang J, Zhang M, *et al.* Achieving high strength and ductility of Al-Cu-Li alloy via creep aging treatment with different pre-strain levels [J]. *Materials Today Communications*, 2021, 29: 102898.
<https://doi.org/10.1016/j.matcomm.2021.102898>
- [13] Chen F, Zhan L, Gao T, *et al.* Creep aging properties variation and microstructure evolution for 2195 Al-Li alloys with various loading rates [J]. *Materials Science and Engineering: A*, 2021, 827: 142055.
<https://doi.org/10.1016/j.msea.2021.142055>
- [14] Xu Y, Zhan L, Ma Z, *et al.* Effect of heating rate on creep aging behavior of Al-Cu-Mg alloy [J]. *Materials Science and Engineering: A*, 2017; 688: 488-497.
<https://doi.org/10.1016/j.msea.2017.02.030>
- [15] Xu L, Tong C, Zhan L, *et al.* Improved creep forming efficiency and retained performance via a novel two-stage creep aging process of Al-Zn-Mg-Cu alloys [J]. *Materials Science and Engineering: A*, 2022; 851: 143581.
<https://doi.org/10.1016/j.msea.2022.143581>
- [16] Chen F, Wang P, Zhan L, *et al.* Creep behavior and microstructure evolution during two-stage creep aging of a 2195 Al-Li alloy [J]. *Materials Science and Engineering: A*, 2022; 850: 143555.
<https://doi.org/10.1016/j.msea.2022.143555>
- [17] Zhan L, Yu W, Xu Y, *et al.* Creep aging behavior of Al-Cu-Mg-Si alloy with elastic and plastic loads [J]. *Materials Characterization*, 2022; 191: 112132.
<https://doi.org/10.1016/j.matchar.2022.112132>
- [18] Chen F, Zhong J, Zhan L, *et al.* Effect of pre-aging on creep aging properties and microstructure evolution of 2195 Al-Li alloy [J]. *Journal of Materials Research and Technology*, 2022; 21: 1029-1041.
<https://doi.org/10.1016/j.jmrt.2022.09.075>
- [19] Chen K, Liu C, Ma P, *et al.* Enhancing creep formability and comprehensive property in Al-Mg-Si alloy by combinatorial pre-ageing and large pre-deformation [J]. *Materials Science and Engineering: A*, 2021; 826: 141967.
<https://doi.org/10.1016/j.msea.2021.141967>
- [20] Dai H, Xu G, Li Y, *et al.* Effects of electropulsing frequency on mechanical properties, corrosion behavior and microstructure of a creep-aged 7050 aluminum alloy [J]. *Materials Characterization*, 2022; 194: 112386.
<https://doi.org/10.1016/j.matchar.2022.112386>
- [21] Zhou C, Zhan L, Li H. Improving creep age formability of an Al-Cu-Li alloy by electropulsing [J]. *Journal of Alloys and Compounds*, 2021; 870: 159482.
<https://doi.org/10.1016/j.jallcom.2021.159482>
- [22] Chen K, Zhan L, Xu Y, *et al.* Effect of pulsed current density on creep-aging behavior and microstructure of AA7150 aluminum alloy [J]. *Journal of Materials Research and Technology*, 2020; 9(6): 15433-15441.
<https://doi.org/10.1016/j.jmrt.2020.10.100>
- [23] Wang X, Rong Q, Shi Z, *et al.* Improved creep behaviour for a high strength Al-Li alloy in creep age forming: Experimental studies and constitutive modelling [J]. *International Journal of Plasticity*, 2022; 159: 103447.
<https://doi.org/10.1016/j.ijplas.2022.103447>
- [24] Peng N, Zhan L, Xu Y, *et al.* Anisotropy in creep-aging behavior of Al-Li alloy under different stress levels: experimental and constitutive modelling [J]. *Journal of Materials Research and Technology*, 2022; 20: 3456-3470.
<https://doi.org/10.1016/j.jmrt.2022.08.046>
- [25] Li Y, Shi Z, Lin J, *et al.* Experimental investigation of tension and compression creep-ageing behaviour of AA2050 with different initial tempers [J]. *Materials Science and Engineering: A*, 2016; 657: 299-308.
<https://doi.org/10.1016/j.msea.2016.01.074>
- [26] Hu L, Zhan L, Liu Z, *et al.* The effects of pre-deformation on the creep aging behavior and mechanical properties of Al-Li-S4 alloys [J]. *Materials Science and Engineering: A*, 2017; 703: 496-502.
<https://doi.org/10.1016/j.msea.2017.07.068>
- [27] Jiang L, Cui Y, Wu M, *et al.* Creep behavior and dislocation mechanism of Ni3Al based single crystal alloy IC6SX at 760° C [J]. *Progress in Natural Science: Materials International*, 2021; 31(5): 755-761.
<https://doi.org/10.1016/j.pnsc.2021.09.006>
- [28] Fernández R, Bruno G, Garcés G, *et al.* Fractional Brownian motion of dislocations during creep deformation of metals [J]. *Materials Science and Engineering: A*, 2020; 796: 140013.
<https://doi.org/10.1016/j.msea.2020.140013>
- [29] Jiang S, Peng R L, Hegedűs Z, *et al.* Micromechanical behavior of multilayered Ti/Nb composites processed by accumulative roll bonding: An in-situ synchrotron X-ray diffraction investigation [J]. *Acta Materialia*, 2021; 205: 116546.
<https://doi.org/10.1016/j.actamat.2020.116546>
- [30] Ungar T. Microstructural parameters from X-ray diffraction peak broadening [J]. *Scripta Materialia*, 2004; 51(8): 777-781.
<https://doi.org/10.1016/j.scriptamat.2004.05.007>
- [31] Zhou C, Zhan L, Li H, *et al.* Mechanism of an acceleration in T1 precipitation kinetics in an Al-Cu-Li alloy by electropulsing [J]. *Vacuum*, 2021; 194: 110558.
<https://doi.org/10.1016/j.vacuum.2021.110558>
- [32] Xu Y, Zhan L, Li W. Effect of pre-strain on creep aging behavior of 2524 aluminum alloy [J]. *Journal of Alloys and Compounds*, 2017; 691: 564-571.
<https://doi.org/10.1016/j.jallcom.2016.08.291>
- [33] Chen K, Wu X, Cao Y, *et al.* Enhanced strength and ductility in an Al-Cu-Li alloy via long-term ageing [J]. *Materials Science and Engineering: A*, 2021; 811: 141092.
<https://doi.org/10.1016/j.msea.2021.141092>
- [34] Vasudevan A K, Ludwiczak E A, Baumann S F, *et al.* Grain boundary fracture in Al-Li alloys [J]. *Materials science and technology*, 1986; 2(12): 1205-1209.
<https://doi.org/10.1179/mst.1986.2.12.1205>
- [35] Suresh S, Vasudevan A K, Tosten M, *et al.* Microscopic and macroscopic aspects of fracture in lithium-containing aluminum alloys [J]. *Acta Metallurgica*, 1987; 35(1): 25-46.
[https://doi.org/10.1016/0001-6160\(87\)90210-0](https://doi.org/10.1016/0001-6160(87)90210-0)
- [36] Jha S C, Sanders Jr T H, Dayananda M A. Grain boundary precipitate free zones in Al-Li alloys [J]. *Acta Metallurgica*, 1987; 35(2): 473-482.
[https://doi.org/10.1016/0001-6160\(87\)90253-7](https://doi.org/10.1016/0001-6160(87)90253-7)

[37] Ren S, Chen J, Liu J, Fang L, Liu P, Ming W, Wu C. Study of grain boundary precipitation behavior of 7150 aluminum alloy during aging [J]. *Journal of Electron Microscopy*, 2011; 30(Z1): 444-450.

[38] Munitz A, Cotler C, Talianker M. Aging impact on mechanical properties and microstructure of Al-6063 [J]. *Journal of materials science*, 2000; 35(10): 2529-2538.
<https://doi.org/10.1023/A:1004742407600>

Received on 10-11-2022

Accepted on 16-12-2022

Published on 26-12-2022

DOI: <https://doi.org/10.31875/2410-4701.2022.09.07>

© 2022 Feng *et al.*; Zeal Press.

This is an open access article licensed under the terms of the Creative Commons Attribution License (<http://creativecommons.org/licenses/by/4.0/>) which permits unrestricted use, distribution and reproduction in any medium, provided the work is properly cited.